Long time behaviour of diffusing particles in constrained geometries; application to chromatin motion

2006 J. Phys.: Condens. Matter 18 S235

(http://iopscience.iop.org/0953-8984/18/14/S08)

INSTITUTE OF PHYSICS PUBLISHING JOURNAL OF PHYSICS: CONDENSED MATTER

J. Phys.: Condens. Matter **18** (2006) S235–S243 doi:10.1088/0953-8984/18/14/S08

Long time behaviour of diffusing particles in constrained geometries; application to chromatin motion

A Rosa[1,4], F R Neumann[2], S M Gasser[2] and A Stasiak[3]

[1] Institut de Mathématiques B, École Polytechnique Fédérale de Lausanne, 1015 Lausanne, Switzerland
[2] Friedrich Miescher Institute for Biomedical Research, 4058 Basel, Switzerland
[3] Laboratoire d'Analyse Ultrastructurale, Bâtiment de Biologie, Université de Lausanne, 1015 Lausanne, Switzerland

E-mail: angelo.rosa@epfl.ch

Received 28 July 2005
Published 24 March 2006
Online at stacks.iop.org/JPhysCM/18/S235

Abstract

Inspired by experiments that use single-particle tracking to measure the regions of confinement of selected chromosomal regions within cell nuclei, we have developed an analytical approach that takes into account various possible positions and shapes of the confinement regions. We show, in particular, that confinement of a particle into a subregion that is entirely enclosed within a spherical volume can lead to a higher limit of the mean radial square displacement value than the one associated with a particle that can explore the entire spherical volume. Finally, we apply the theory to analyse the motion of extrachromosomal chromatin rings within nuclei of living yeast.

1. Introduction

In recent years, single-particle tracking (SPT) has become a powerful tool for characterizing the mechanisms of particle motion in living cells and in other systems [1–4]. SPT was used to extract information about diffusion coefficients and other transport properties in small systems and give an estimate of the volume accessible to a diffusing particle [1].

Let us briefly review some facts about diffusion.

The main property of a diffusing particle in an infinite medium is that the average square displacement $\Delta d^2(t)$ defined as

$$\Delta d^2(t) = \langle [\mathbf{r}(t) - \mathbf{r}(0)]^2 \rangle \tag{1}$$

[4] Author to whom any correspondence should be addressed.

is proportional to time t [5]. In equation (1), $\mathbf{r}(0)$ and $\mathbf{r}(t)$ are the positions of the particle at the initial time 0 and at t, respectively. The average in equation (1) is an *ensemble* average and can be written as

$$\Delta d^2(t) = \int\int P(\mathbf{r}')(\mathbf{r}-\mathbf{r}')^2 P(\mathbf{r}|\mathbf{r}', t)\,\mathrm{d}\mathbf{r}\,\mathrm{d}\mathbf{r}', \tag{2}$$

where $P(\mathbf{r})$ is the steady-state distribution of particle position and $P(\mathbf{r}|\mathbf{r}', t)$ is the transition probability, i.e., the probability that a particle originally at $\mathbf{r}'$ will be at $\mathbf{r}$ after a time period t.

If the process is at equilibrium the ensemble average may be computed as a time average over a single trajectory [5, 6]. Therefore,

$$\Delta d^2(t) = \int_{t'} |\mathbf{r}(t+t') - \mathbf{r}(t')|^2\,\mathrm{d}t'. \tag{3}$$

Equation (3) is particularly suitable for experiments. For a finite set of N measurements $\{\mathbf{r}_i, i = 1, \ldots, N\}$, equation (3) becomes

$$\Delta d^2(t) = \Delta d^2(\mathrm{i}\Delta t) = \frac{1}{N-i}\sum_{i'=1}^{N-i} |\mathbf{r}_{i+i'} - \mathbf{r}_{i'}|^2 \tag{4}$$

where $t = \mathrm{i}\Delta t$, Δt being the acquisition time interval.

Interestingly, if the system is finite sized, Δd^2 is no longer proportional to t for $t \to \infty$, but $\Delta d^2(\infty)$ remains finite and can be used to measure the confinement volume accessible to a diffusing particle. We assume here that within the region of confinement every position can be visited with the same probability, as is the case for a gas of molecules in a container. If the time interval between two registered positions of a tracked particle ($\mathbf{r}_1$ and $\mathbf{r}_2$) is sufficiently long, there is no correlation between the two positions. Then, $\Delta d^2(\infty)$ can be calculated as an *ensemble* average over an equilibrium distribution.

The long time limit of equation (1) is therefore

$$\Delta d^2(\infty) = \langle(\mathbf{r}_2 - \mathbf{r}_1)^2\rangle_{12}, \tag{5}$$

where $\langle\cdot\rangle_{12}$ means an average over the joint distribution for two random positions $\mathbf{r}_1$ and $\mathbf{r}_2$, respectively. Since the two positions are independent, this distribution is simply the product of the one-particle distributions for particle 1 and particle 2. From equation (5), it turns out that

$$\Delta d^2(\infty) = 2(\langle\mathbf{r}^2\rangle - \langle\mathbf{r}\rangle^2), \tag{6}$$

where now the average is performed over the one-particle distribution and the particle is taken at position $\mathbf{r}$.

It should be stressed here that although equation (1) provides the standard treatment of a diffusing system, true experimental conditions force researchers to switch to other ways of monitoring the positions of tracked particles. In particular, several recent papers [7–9], focusing on the dynamics of chromosomes in yeast interphase nuclei, have pointed out that rotation of the cellular nucleus can be a serious problem for the experimentalist. To compensate for possible effects of rotation, the radial distance from the centre of the nucleus to the monitored locus was measured, as this does not change upon rotation of a quasi-spherical cell nucleus [7, 8]. Therefore, movements of tracked particles are defined in terms of radial displacement

$$\Delta d_{\mathrm{r}}^2(t) = \langle[r(t) - r(0)]^2\rangle \tag{7}$$

instead of equation (1). In equation (7), $r(t)$ and $r(0)$ are the distances of the particles from the reference point. We call $\Delta d_{\mathrm{r}}^2(t)$ the mean radial square displacement. For a finite set of N measurements, analogously to equation (4), we have

$$\Delta d_{\mathrm{r}}^2(t) = \Delta d_{\mathrm{r}}^2(\mathrm{i}\Delta t) = \frac{1}{N-i}\sum_{i'=1}^{N-i} |r_{i+i'} - r_{i'}|^2. \tag{8}$$

Again, at long time, for a particle enclosed in a spherical confinement region, $\Delta d_r^2(t)$ takes a finite value, namely $\Delta d_r^2(\infty)$, where

$$\Delta d_r^2(\infty) = 2(\langle r^2 \rangle - \langle r \rangle^2). \tag{9}$$

Nevertheless, it should be stressed that $\Delta d_r^2(\infty)$ depends not only on the size of the spherical region of confinement, but also on the distance between the reference point and the centre of the spherical region of confinement.

This paper is organized as follows. In section 2, we present computations of equation (9) for some simple geometries. In section 3, we discuss some possible biological applications.

2. Computation of $\Delta d_r^2(\infty)$ in simple geometries

2.1. 3D case

As the first simple example we consider the case of a freely diffusing particle within a sphere of radius R. We choose a reference frame whose origin coincides with the centre of the sphere. This is relevant for biological experiments that measure confinement regions within cellular nuclei of roughly spherical shape. In these cases, nuclear centres are taken as convenient reference points for the measurements of mean radial displacements of tracked particles [7–11].

It is clear that, at equilibrium, the distribution of the freely diffusing particle is, simply,

$$P(\boldsymbol{\rho}) = P(\rho) = 1/V, \tag{10}$$

where $\boldsymbol{\rho}$ is the vector pointing to the particle and $V = \frac{4}{3}\pi R^3$ is the volume of the sphere. In this case, the average square displacement $\Delta d_r^2(\infty)$ is

$$\frac{\Delta d_r^2(\infty)}{R^2} = \frac{3}{40} = 0.075. \tag{11}$$

This result tells us that, in the case where the confinement volume is spherical and the centre of the confinement sphere is taken as the reference point, $\Delta d_r^2(\infty)$ amounts to $0.075R^2$, with R being the radius of the sphere of confinement.

Let us consider now the case where the sphere of confinement is not centred around the origin of the reference frame. In fact, such a situation was assumed to be the case in the studies of chromosomal confinement by Marshall *et al* [10]. For our derivation, we consider the shift over a distance d along the y-axis (see the inset in figure 1), but, of course, a shift in any other direction over distance d would give the same result for $\Delta d_r^2(\infty)$.

The equation of the sphere, in the frame shown in figure 1, is $x^2 + (y-d)^2 + z^2 = R^2$. So, the probability distribution $\pi(x, y, z)$ for a particle uniformly distributed in the sphere is

$$\pi(x, y, z) \propto \Theta[R^2 - (x^2 + (y-d)^2 + z^2)], \tag{12}$$

where $\propto$ stands for proportionality and $\Theta(x)$ is the Heaviside step function. It is convenient to introduce a frame of spherical coordinates (ρ, θ, ϕ) defined as $(x, y, z) = (\rho \sin\theta \sin\phi, \rho\cos\theta, \rho \sin\theta \cos\phi)$. Since we are mainly interested in $\langle\rho\rangle$ and $\langle\rho^2\rangle$ (see equation (9)), we calculate the reduced distribution $P(\rho)$ obtained by integrating over the irrelevant variables θ and ϕ. From equation (12), we get

$$P(\rho) \propto \int_0^\pi \Theta(R^2 - d^2 + 2\,\mathrm{d}\rho\cos\theta - \rho^2)\sin\theta\,\mathrm{d}\theta. \tag{13}$$

There are two different cases: $0 \leqslant d/R \leqslant 1$ and $1 < d/R$. After some tedious algebra, we obtain

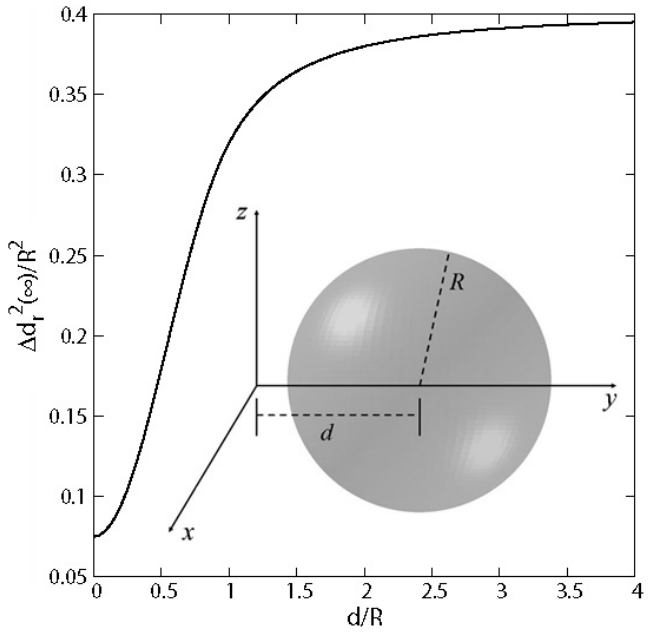

Figure 1. Plot of $\Delta d_r^2(\infty)/R^2$ (see equation (9)) versus d/R. Here, $\langle\rho\rangle/R$ and $\langle\rho^2\rangle/R^2$ are described by equations (16) and (17) for $0 \leqslant d/R \leqslant 1$ and $1 < d/R$, respectively. Inset: the volume available for the diffusing particle is a sphere of radius R whose centre has coordinates $(0, d, 0)$.

(i) $0 \leqslant d/R \leqslant 1$

$$P(\rho) \propto \begin{cases} 2 & \text{if } 0 \leqslant \rho \leqslant R-d \\ 1 - \dfrac{\rho^2 - R^2 + d^2}{2d\rho} & \text{if } R-d \leqslant \rho \leqslant R+d \\ 0 & \text{otherwise,} \end{cases} \tag{14}$$

(ii) $1 < d/R$

$$P(\rho) \propto \begin{cases} 1 - \dfrac{\rho^2 - R^2 + d^2}{2d\rho} & \text{if } d-R \leqslant \rho \leqslant d+R \\ 0 & \text{otherwise.} \end{cases} \tag{15}$$

Then, defining $x = d/R$, from equations (14) and (15) we derive the final results:

(i) $0 \leqslant x \leqslant 1$

$$\begin{aligned} \frac{\langle\rho\rangle}{R} &= \frac{3}{2}(1+x)^4\left[\frac{1}{4} - \frac{1+x}{10x}\left(1 - \left(\frac{1-x}{1+x}\right)^5\right)\right. \\ &\quad \left. + \frac{1}{6x}\left(\frac{1-x}{1+x}\right)\left(1 - \left(\frac{1-x}{1+x}\right)^3\right) + \frac{1}{4}\left(\frac{1-x}{1+x}\right)^4\right] \\ \frac{\langle\rho^2\rangle}{R^2} &= \frac{3}{2}(1+x)^5\left[\frac{1}{5} - \frac{1+x}{12x}\left(1 - \left(\frac{1-x}{1+x}\right)^6\right)\right. \\ &\quad \left. + \frac{1}{8x}\left(\frac{1-x}{1+x}\right)\left(1 - \left(\frac{1-x}{1+x}\right)^4\right) + \frac{1}{5}\left(\frac{1-x}{1+x}\right)^5\right]. \end{aligned} \tag{16}$$

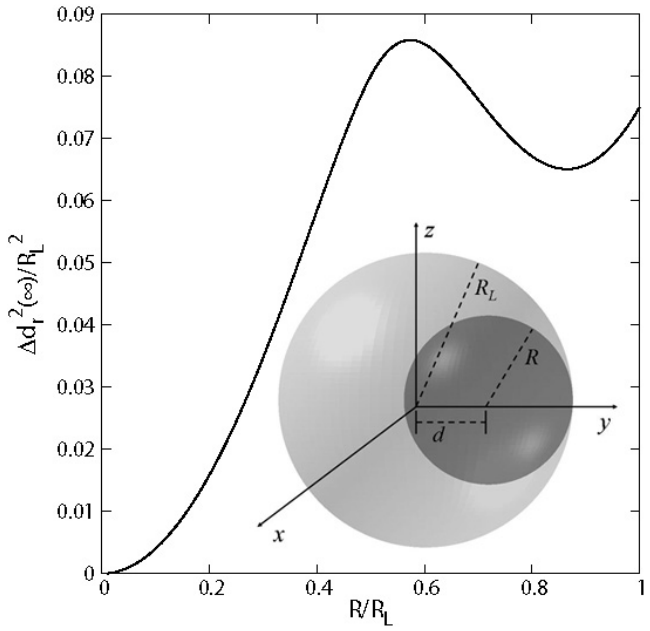

Figure 2. Plot of $\Delta d_r^2(\infty)/R_L^2$ (see equation (9)) versus R/R_L. Here, $\langle\rho\rangle/R_L$ and $\langle\rho^2\rangle/R_L^2$ are described by equations (18) and (19) for $0 \leqslant R/R_L \leqslant 1/2$ and $1/2 < R/R_L \leqslant 1$, respectively. Inset: the volume available for the diffusing particle is a sphere of radius R, internally tangent to a larger sphere of radius R_L. The origin of the chosen frame coincides with the centre of the large sphere.

(ii) $1 < x$

$$\begin{aligned}\frac{\langle\rho\rangle}{R} &= \frac{3}{20}(1+x)^3\left[1-\frac{5}{3}\left(\frac{x-1}{x+1}\right)+\left(\frac{x-1}{x+1}\right)^2\right.\\ &\quad\left.+\,5\left(\frac{x-1}{x+1}\right)^3-\frac{16}{3}\frac{x+1/4}{x}\left(\frac{x-1}{x+1}\right)^3\right]\\ \frac{\langle\rho^2\rangle}{R^2} &= \frac{1}{10}(1+x)^4\left[1-\frac{3}{2}\left(\frac{x-1}{x+1}\right)+\left(\frac{x-1}{x+1}\right)^2\right.\\ &\quad\left.-\,\frac{3}{2}\left(\frac{x-1}{x+1}\right)^3+\left(\frac{x-1}{x+1}\right)^4\right].\end{aligned} \tag{17}$$

Finally, $\Delta d_r^2(\infty)$ can be derived from equation (9). The result is plotted in figure 1.

We observe two striking features: (a) the curve is monotonically increasing; (b) in the limit $d \to \infty$, $\Delta d_r^2(\infty)$ reaches the asymptotic value of $2/5R^2 = 0.4R^2$, where R is the radius of the sphere of confinement.

The former observation turns out to be important once we embed a sphere of confinement (of radius R), e.g. a chromosomal territory, within a larger sphere (of radius R_L), e.g. the cellular nucleus (see the inset in figure 2) [7]. Because of the monotonic character of the curve plotted in figure 1, it is readily concluded that for any fixed R of the embedded sphere the highest $\Delta d_r^2(\infty)$ value is obtained when the embedded sphere is tangential to the embedding sphere.

Let us consider now what is the highest possible limit of $\Delta d_r^2(\infty)$ for the situation of two tangential spheres where one encloses the other (as in the case of a spherical chromosomal territory in a cell nucleus). In addition to finding the limit of $\Delta d_r^2(\infty)$, we are interested in finding the ratio of the radii of the embedded and embedding spheres that maximizes $\Delta d_r^2(\infty)$.

The function $\Delta d_{\mathrm{r}}^2(\infty)/R_L^2$ can be derived from equations (16) and (17) with the substitution $d = R_L - R$ (see the inset in figure 2). Now defining $x = R/R_L$, the final result reads

(i) $0 \leqslant x \leqslant 1/2$

$$\frac{\langle\rho\rangle}{R_L} = \frac{3}{20x^2}\left[1 - \frac{5}{3}(1-2x) + (1-2x)^2 + 5(1-2x)^3 - \frac{16}{3}\frac{1-3x/4}{1-x}(1-2x)^3\right]$$
$$\frac{\langle\rho^2\rangle}{R_L^2} = \frac{1}{10x^2}\left[1 - \frac{3}{2}(1-2x) + (1-2x)^2 - \frac{3}{2}(1-2x)^3 + (1-2x)^4\right]. \tag{18}$$

(ii) $1/2 < x \leqslant 1$

$$\frac{\langle\rho\rangle}{R_L} = \frac{3}{2x^3}\left[\frac{1}{4} - \frac{1-(2x-1)^5}{10(1-x)} + \frac{1}{4}(2x-1)^4 - \frac{1-2x}{6(1-x)}(1-(2x-1)^3)\right]$$
$$\frac{\langle\rho^2\rangle}{R_L^2} = \frac{3}{2x^3}\left[\frac{1}{5} - \frac{1-(2x-1)^6}{12(1-x)} + \frac{1}{5}(2x-1)^5 - \frac{1-2x}{8(1-x)}(1-(2x-1)^4)\right]. \tag{19}$$

The plot of $\Delta d_{\mathrm{r}}^2(\infty)/R_L^2$ versus R/R_L is shown in figure 2. Let us remark that the curve has a non-trivial behaviour, reaching the maximum 0.0858 . . . for $R/R_L \simeq 0.573\,48\ldots$. This maximum is larger than 0.075, i.e. the value obtained when the confining region coincides with the larger sphere (see above).

Figure 2 demonstrates that a confinement into a spherical subregion can in fact increase the $\Delta d_{\mathrm{r}}^2(\infty)$ value as compared to the $\Delta d_{\mathrm{r}}^2(\infty)$ value in a larger enclosing sphere. The increase of $\Delta d_{\mathrm{r}}^2(\infty)$ is however a modest one and could be not recognized in real biological experiments.

Let us consider now the effect of other possible shapes of the regions of confinement within a spherical enclosing volume. Since the chromosomal territories are likely to be elongated [11–13], we consider here the case of cylindrical subregions within an enclosing sphere.

A rather simple configuration that could capture these features is sketched in the inset of figure 3. As explained in the caption, the volume available for the diffusing particle is the one obtained from the intersection of the sphere of radius R and the infinite cylinder of radius r. We mean to preserve the symmetry around the z-axis, but, again, any other position would lead to the same result.

It is convenient to choose a frame of cylindrical coordinates $(\rho_\perp, \phi, \rho_\parallel)$ defined as $(x, y, z) = (\rho_\perp \cos\phi, \rho_\perp \sin\phi, \rho_\parallel)$.

The probability distribution $P(\rho_\perp, \rho_\parallel)$ for a particle uniformly distributed inside the volume described above is

$$P(\rho_\perp, \rho_\parallel) \propto \Theta[{\rho_\parallel}^2 - (R^2 - r^2)]\Theta[-{\rho_\perp}^2 + (R^2 - {\rho_\parallel}^2)] + \Theta[-{\rho_\parallel}^2 + (R^2 - r^2)]\Theta(-{\rho_\perp}^2 + r^2). \tag{20}$$

Now, to compute $\Delta d_{\mathrm{r}}^2(\infty)$, we must face the averages $\langle\rho\rangle = \left\langle\sqrt{{\rho_\perp}^2 + {\rho_\parallel}^2}\right\rangle$ and $\langle\rho^2\rangle = \langle{\rho_\perp}^2 + {\rho_\parallel}^2\rangle = \langle{\rho_\perp}^2\rangle + \langle{\rho_\parallel}^2\rangle$.

We get

$$\frac{\langle\rho\rangle}{R} = \frac{2}{3N(x)}\left\{\frac{1}{8}\left[2\sqrt{1-x^2}\left(1 + \frac{3x^2}{2}\right) + 3x^4 \log\left(\frac{1+\sqrt{1-x^2}}{x}\right)\right] + \frac{3}{4} - \sqrt{1-x^2}\right\}$$
$$\frac{\langle\rho^2\rangle}{R^2} = \frac{2}{5N(x)}\left[1 - \left(1 + \frac{2x^2}{3}\right)(1-x^2)^{3/2}\right] \tag{21}$$

where $N(x) = \frac{2}{3}[1 - (1-x^2)^{3/2}]$ and $x = r/R$.

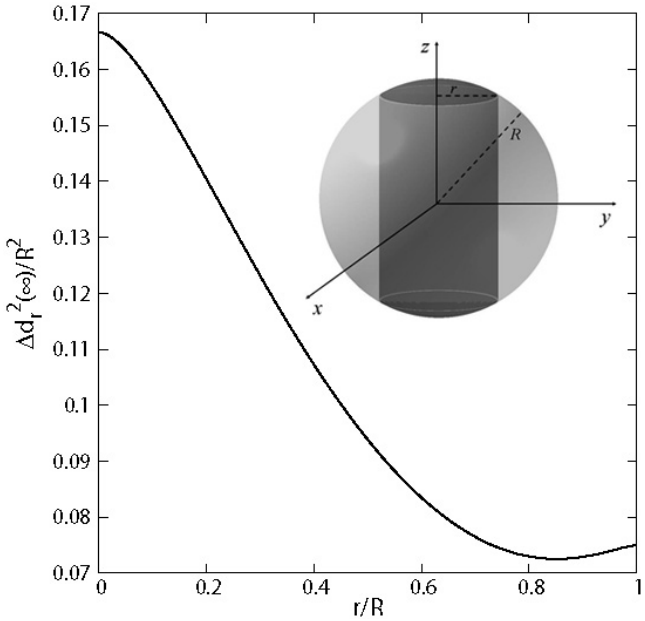

Figure 3. Plot of $\Delta d_r^2(\infty)/R^2$, equation (9), where $\langle\rho\rangle/R$ and $\langle\rho^2\rangle/R^2$ are described by equation (21). Inset: the volume available for the diffusing particle is obtained from the geometrical intersection of a sphere of radius R and an infinite cylinder whose radius is $r < R$. The origin of the chosen frame coincides with the centre of the sphere.

Again, $\Delta d_r^2(\infty)$ can be derived from equation (9). The final result is plotted in figure 3.

A comparison with figure 2 shows that a confinement to a cylindrical subregion can lead to a much higher $\Delta d_r^2(\infty)$ than a confinement to a spherical subregion. In particular, for $r = 0$, $\Delta d_r^2(\infty)/R^2 = 1/6 \simeq 0.1666\ldots$.

2.2. 2D case

In real biological experiments that use confocal microscopy to track movements of chromosomal regions [7–9], the measurements of z coordinates are prone to higher errors than the measurements of x and y coordinates. Therefore, researchers frequently rely on just the projected radial distances of tracked chromosomal loci on an imagined equatorial plane of the nucleus. The 2D radial square displacement now reads

$$\Delta d_{r,2D}^2(t) = \langle [r_\perp(t) - r_\perp(0)]^2 \rangle \tag{22}$$

where $r_\perp$ is the norm of the orthogonal projection of $\mathbf{r}$ on the plane of measurement. The long time limit of equation (22) is (see also equation (9))

$$\Delta d_{r,2D}^2(\infty) = 2(\langle r_\perp^2 \rangle - \langle r_\perp \rangle^2). \tag{23}$$

Moreover, the analogue of equation (8) is given by

$$\Delta d_{r,2D}^2(t) = \Delta d_{r,2D}^2(i\Delta t) = \frac{1}{N-i} \sum_{i'=1}^{N-i} |r_{\perp,i+i'} - r_{\perp,i'}|^2, \tag{24}$$

where $r_{\perp,i} = \sqrt{x_i^2 + y_i^2}$, x_i and y_i being the coordinates of the tracked site with respect to the centre of the nucleus, recorded at the time $t = i\Delta t$.

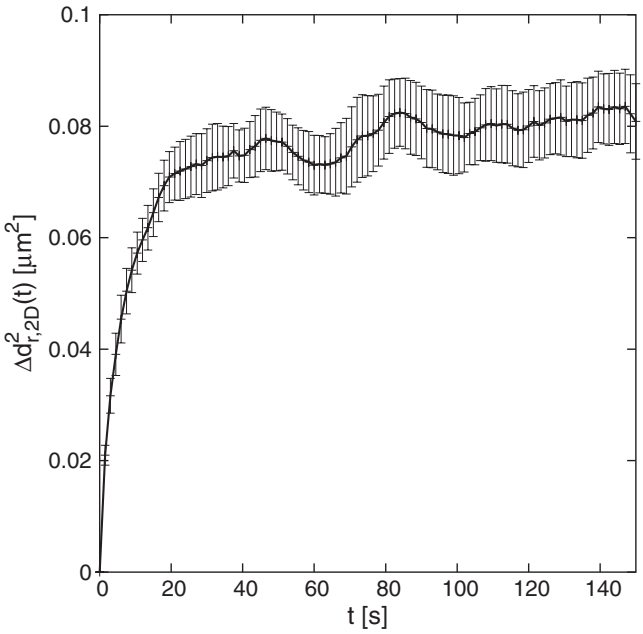

Figure 4. Plot of $\Delta d^2_{\mathrm{r,2D}}(t)$ versus t (continuous line), measured for the extrachromosomal chromatin rings (*LYS2*) in yeast nuclei [9]. The vertical bars correspond to the statistical standard deviations calculated for each time t over nine independent experimental realizations. The function $\Delta d^2_{\mathrm{r,2D}}(\infty)[1 - \exp(-t/\tau)]$ is fitted to the continuous line with a plateau value $\Delta d^2_{\mathrm{r,2D}}(\infty) \simeq 0.08\ \mu\mathrm{m}^2$, corresponding to a radius of confinement of $\simeq 0.85\ \mu$m, equation (25).

As an example, we calculate explicitly equation (23) for the simple configuration shown in the inset of figure 1, i.e. we are again supposing that the region of confinement is a sphere whose equatorial plane coincides with the plane of observation. Let us remark that this is a serious approximation, since the region of confinement could be found anywhere inside the nucleus. Nevertheless, we think that this is a nice case study, since it shows some features of the confinement in real experiments (see section 3). Again, for a sphere whose centre coincides with the centre of the frame, we have the exact result

$$\frac{\Delta d^2_{\mathrm{r,2D}}(\infty)}{R^2} = 2\left[\frac{2}{5} - \left(\frac{3\pi}{16}\right)^2\right] \simeq 0.106. \tag{25}$$

This result tells us that, in the case where the confinement volume is spherical and the centre of the confinement sphere is taken as the reference point, $\Delta d^2_{\mathrm{r,2D}}(\infty)$ amounts to $\sim 0.106 R^2$, with R being the radius of the sphere of confinement.

3. Biological applications

Figure 4 shows the behaviour of $\Delta d^2_{\mathrm{r,2D}}(t)$, equation (24), measured for the extrachromosomal chromatin rings (*LYS2*) in yeast nuclei [9] (continuous line).

The plot is obtained as an average over nine independent experimental realizations, each of them consisting of $\sim$300 data points, acquired every $\Delta t = 1.5$ s. The vertical bars are the corresponding statistical standard deviations. It can be seen that as the time interval between the measured positions increases, the $\Delta d^2_{\mathrm{r,2D}}(t)$ reaches the plateau value $\Delta d^2_{\mathrm{r,2D}}(\infty)$

of $\simeq 0.08\ \mu m^2$, which is obtained by fitting the function $\Delta d^2_{r,2D}(\infty)[1 - \exp(-t/\tau)]$ to the continuous line.

This value indicates that the extrachromosomal chromatin rings behave as if freely diffusing within a sphere of $\simeq 0.85\ \mu m$ radius, equation (25). Since the radius of the yeast nuclei is $\simeq 0.9\ \mu m$ in the G_1 phase of the cell cycle [9], we conclude that *LYS2* rings can explore the entire volume of the nucleus.

It is important to add here that independent experiments using a photobleaching approach demonstrated that on the timescale of the experiment the observed nuclei do not show a significant overall rotation [14]. Therefore, the $\Delta d^2_{r,2D}(\infty)$ value of $\simeq 0.08\ \mu m^2$ is primarily due to a free diffusion of *LYS2* rings within yeast nuclei.

This analysis agrees with an earlier study where a different formalism based on the 2D version of equation (5) was used [9]. Let us remark, however, that in the case of a uniform distribution within a sphere of radius R, $\Delta d^2_{2D}(\infty) = 0.8R^2$.

4. Conclusions

We described here a theoretical treatment based on $\Delta d^2_r(\infty)$ and $\Delta d^2_{r,2D}(\infty)$ for analysing the diffusion of tracked particles in constrained geometries. We have analysed the effect of the shape of the region of the confinement on the $\Delta d^2_r(\infty)$. We have applied the formalism developed to study the motion of extrachromosomal chromatin rings in nuclei of living yeast. The analysis indicates that extrachromosomal chromatin fragments are free to diffuse within the entire volume of the nuclei studied.

Acknowledgments

We thank J Dubochet and J H Maddocks for useful discussions.

The research was partially sponsored by Grants No 3152-68151.02 and 3100A0-103962.

Work in the Gasser laboratory is supported by SNF grant 3100-061605/2, NCCR Frontiers in Genetics and the NOE Epigenome.

References

[1] Qian H, Sheetz M P and Elson E L 1991 *Biophys. J.* **60** 910
[2] Carlsson A E, Shah A D, Elking D, Karpova T S and Cooper J A 2002 *Biophys. J.* **82** 2333
[3] Ritchie K and Kusumi A 2003 *Methods Enzymol.* **360** 618
[4] Suh J, Dawson M and Hanes J 2005 *Adv. Drug Deliver. Rev.* **57** 63
[5] Chandrasekhar S 1943 *Rev. Mod. Phys.* **15** 1
[6] Huang K 1987 *Statistical Mechanics* 2nd edn (New York: Wiley)
[7] Heun P, Laroche Th, Shimada K, Furrer P and Gasser S M 2001 *Science* **294** 2181
[8] Gasser S M 2002 *Science* **296** 1412
[9] Gartenberg M R, Neumann F R, Laroche Th, Blaszczyk M and Gasser S M 2004 *Cell* **119** 955
[10] Marshall W F, Straight A, Marko J F, Swedlow J, Dernburg A, Belmont A, Murray A W, Agard D A and Sedat J W 1997 *Curr. Biol.* **7** 930
[11] Marshall W F, Fung J C and Sedat J W 1997 *Curr. Opin. Genet. Dev.* **7** 259
[12] Rabl C 1885 *Morphologisches Jahrbuch* **10** 214
[13] Comings D 1968 *Am. J. Hum. Genet.* **20** 550
[14] Bystricky K, Laroche Th, van Houwe G, Blaszczyk M and Gasser S M 2005 *J. Cell Biol.* **168** 375